

ROBUST FIBER RESPONSE FUNCTION ESTIMATION FOR DECONVOLUTION BASED DIFFUSION MRI METHODS

Chantal M.W. Tax¹, Ben Jeurissen², Max A. Viergever¹, and Alexander Leemans¹

¹Image Sciences Institute, University Medical Center Utrecht, Utrecht, Netherlands, ²Department of Physics, University of Antwerp, iMinds-Vision Lab, Antwerp, Belgium

Introduction: There is accumulating evidence that at current acquisition resolutions for diffusion-weighted (DW) MRI, the vast majority of white matter (WM) voxels contains "crossing fibers", referring to complex fiber configurations, in which multiple and distinctly differently oriented fiber populations exist [1]. During the last decade, several approaches have been developed to characterize this DW intra-voxel signal heterogeneity in great detail. Spherical deconvolution (SD) based techniques, in particular, are quite appealing as they provide a balanced trade-off between constraints on the required hardware performance and acquisition time on the one hand, and the reliability of the reconstructed fiber orientation distribution (FOD) function on the other hand [2]. Recent findings, however, suggest that an inaccurate calibration of the response function (RF), which represents the DW signal profile of a single and straight fiber bundle, can lead to the detection of spurious FOD peaks which severely impacts tractography results [3]. Currently, the computation of this RF is either model based or estimated from selected voxels that have a fractional anisotropy (FA) above a predefined threshold. Defining an FA threshold, for instance, influences the FOD peak orientations as shown in Fig. 1. In this work, the computation of the RF is optimized by excluding "crossing fibers" voxels in a recursive framework. By doing so, the fiber response function can be estimated in a robust and automated way without the need for defining ad-hoc FA threshold settings.

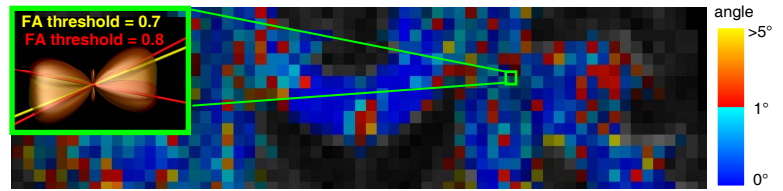


Fig. 1: angle between the dominant peak orientations obtained with FA threshold 0.7 and 0.8

Methods:

Recursive response function estimation: Our framework consists of the following steps: 1) Perform constrained SD (CSD, $l_{max}=8$) [2] in each selected voxel using the RF of previous step. The first iteration was performed with a "fat" response function. For human data, all WM voxels were selected according to a WM mask constructed from the T_1 image [1]; 2) Calculate direction and magnitude of FOD peaks using a Newton optimization algorithm [1]; 3) Select voxels in which the second peak is absent or sufficiently small (below noise level) compared to the first peak; 4) Reorient DW signals in the voxels obtained in step 3) according to the main fiber direction (largest FOD peak); 5) Calculate the new RF from these reoriented DW signals and constrain it to be axially symmetric.

Simulations: Noise free DW data were generated assuming axially symmetric diffusion tensor profiles for each fiber population. For investigating performance and convergence of our algorithm as function of angle and volume fractions (VF), a data set with ratio two-fiber versus one-fiber populations of 9:1 was simulated [1], with $FA=0.8$ for each fiber population. Rician noise was added ($SNR=22$, defined on $b=0$ image), and the "FA of the RF" was estimated by fitting a tensor to the RF. In a second simulation, a data set was created with 10% one-, 45% two- and 45% three-fiber populations. The VF values, inter-fiber angles and FA values were sampled from a Gaussian distribution akin to the distributions obtained in [1] for real human data. Here, multiple levels of Rician noise were added ($SNR=10, 15, 22$ and 30).

Acquisition and image-processing human data: A DW data set (acquired with 2 mm isotropic resolution) was collected on a 3T MR scanner with a gradient sampling scheme consisting of one non-DW image and 60 DW images ($b = 2500$ s/mm²) with the gradient directions uniformly distributed over the sphere [5]. Estimated SNR is 22, and the dataset was corrected for subject motion and eddy currents [6] with *ExploreDTI* [7].

Results:

Simulations: Fig. 2 shows the FA of the RF as function of the iteration steps for the first simulation set for different VF values (a) and angles (b). Voxels were selected when the magnitude of the second largest peak was smaller than 1% compared to the largest peak ("peak threshold" 0.01). For angles of 45° and smaller, one can see that the two-fiber voxels cannot be distinguished from one-fiber voxels and, therefore, will also be selected for RF estimation, which results in a "fatter" RF and thus lower FA. Fig. 3 displays results of the second simulation: (a) shows the sensitivity of the FA threshold method against the number of false positives for feasible thresholds FA threshold [0.6 0.7 0.8 0.9], for different SNR (colored lines). An FOD peak is termed "true positive" when it has an angle difference smaller than $\cos^{-1}(0.95) \approx 18^\circ$ with a true simulated fiber [8]. Fig. 3 (b) shows the same graph for the recursive method, where the second peak should not be smaller than [0.2 0.1 0.05 0.02 0.01 0.005] times the first peak in order to select it as "one fiber voxel" for RF calibration.

Human data: Fig. 4 displays FOD glyphs in the centrum semiovale with the FA threshold method (a) and recursive method (b). Despite the qualitative similarities, significant angular deviations between the dominant peak orientations obtained with both methods can be observed (c).

Discussion and Conclusion: In this work, we presented a recursive method to estimate the RF for SD approaches that does not rely on DTI measures anymore. Our recursive method yields less false positive FOD peaks and the dependence on the threshold in high SNR range is negligible.

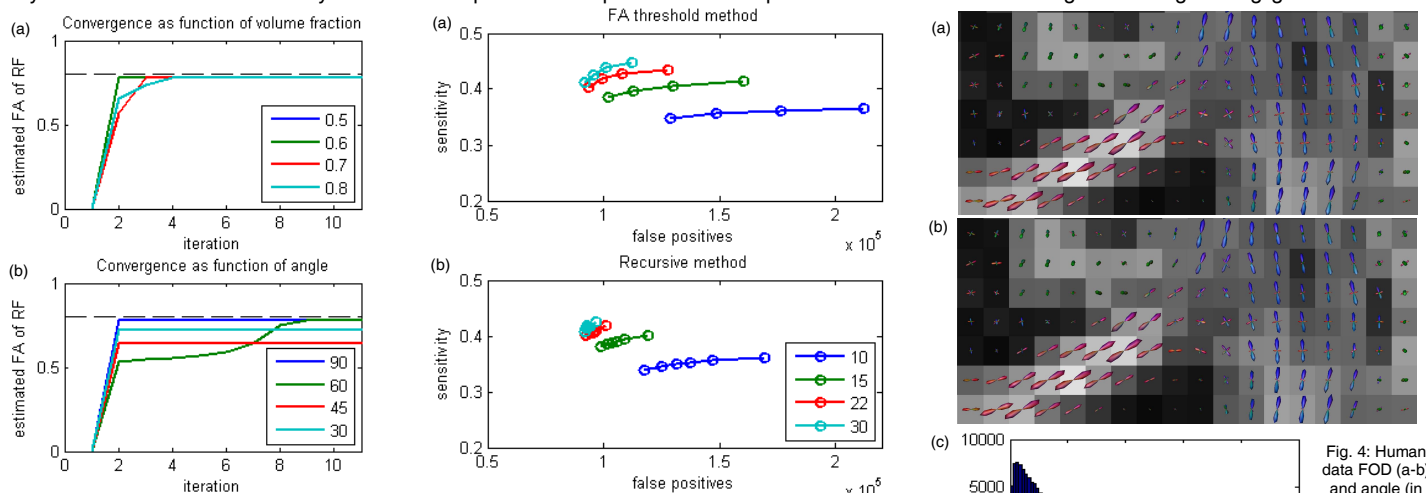


Fig. 2: FA of RF over iteration for (a) different VF with angle 90°, (b) different angles with VF 0.5. Dashed line represents FA 0.8 of simulated fiber population.

Fig. 3: Sensitivity over # false positives for different SNR. (a) FA threshold method with FA [0.6 0.7 0.8 0.9], (b) recursive method with peak threshold [0.2 0.1 0.05 0.02 0.01 0.005]

Fig. 4: Human data FOD (a-b) and angle (in deg) between dominant peaks from both methods (c).

References: [1] Jeurissen et al, HBM, in press: doi: 10.1002/hbm.22099; [2] Tournier et al, NeuroImage 35:1459-1472, 2007; [3] Parker et al, NeuroImage, in press: doi: 10.1016/j.neuroimage.2012.10.022; [4] Sijbers et al, MRM 51:586-594, 2004; [5] Jones et al, MRM 42:515-525, 1999; [6] Leemans et al, MRM 61:1336-1349, 2009; [7] www.ExploreDTI.com; [8] Alexander, Ann N Y Acad Sci 1064:113-33, 2005;